Block of Muscle Nicotinic Receptors by Choline Suggests that the Activation and Desensitization Gates Act as Distinct Molecular Entities

Yamini Purohit and Claudio Grosman

Department of Molecular and Integrative Physiology, Center for Biophysics and Computational Biology, and Neuroscience Program, University of Illinois at Urbana-Champaign, Urbana, IL 61801

Ion channel block in muscle acetylcholine nicotinic receptors (AChRs) is an extensively reported phenomenon. Yet, the mechanisms underlying the interruption of ion flow or the interaction of the blocker with the channel's gates remain incompletely characterized. In this paper, we studied fast channel block by choline, a quaternary-ammonium cation that is also an endogenous weak agonist of this receptor, and a valuable tool in structure–function studies. Analysis of the single-channel current amplitude as a function of both choline concentration and voltage revealed that extracellular choline binds to the open-channel pore with millimolar apparent affinity ($K_B \cong 12$ mM in the presence of ~155 mM monovalent and 3.5 mM divalent, inorganic cations), and that it permeates the channel faster than acetylcholine. This, together with its relatively small size (~5.5 Å along its longest axis), suggests that the pore-blocking choline binding site is the selectivity filter itself, and that current blockages simply reflect the longer-lived sojourns of choline at this site. Kinetic analysis of single-channel traces indicated that increasing occupancy of the pore-blocking site by choline (as judged from the reduction of the single-channel current amplitude) is accompanied by the lengthening of (apparent) open interval durations. Consideration of a number of possible mechanisms firmly suggests that this prolongation results from the local effect of choline interfering with the operation of the activation gate (closure of blocked receptors is slower than that of unblocked receptors by a factor of ~13), whereas closure of the desensitization gate remains unaffected. Thus, we suggest that these two gates act as distinct molecular entities. Also, the detailed understanding gained here on how choline distorts the observed open-time durations can be used to compensate for this artifact during activation assays. This correction is necessary if we are to understand how choline binds to and gates the AChR.

The Journal of General Physiology

INTRODUCTION

The ion channel pore of muscle nicotinic receptors (AChRs) can be blocked by a variety of molecules ranging from simple, monoatomic divalent cations (Imoto et al., 1988) to complex organic molecules like procaine (Adams, 1977), lidocaine derivatives (Neher and Steinbach, 1978), curare derivatives (Katz and Miledi, 1978; Colquhoun et al., 1979), and philanthotoxins (van Wilgenburg et al., 1984). Because pore blockers bind to the inner lining of the pore, they have been extensively used as structural probes of the pore domain (Giraudat et al., 1986; Leonard, et al., 1988; White and Cohen, 1992). Also, the phenomenon of channel block by ACh has been proposed to govern the time course of the endplate current (Legendre et al., 2000), although this considerable departure from the traditional view of neuromuscular synaptic transmission (Edmonds et al., 1995) has been recently challenged (Wen and Brehm, 2005). Another reason why the study of AChR block has elicited interest is that many positively charged agonists of this receptor channel bind to (and block) the pore domain with an affinity that does not differ much from the affinity of the transmitter binding sites for these molecules (Sine and Steinbach, 1984; Ogden and Colquhoun, 1985; Carter and Oswald, 1993; Maconochie and Steinbach, 1995). As a direct result of this, blockade often interferes with studies of the activation of the channel, becoming a "nuisance" that needs to be understood in some detail for its effect to be correctly compensated. Yet another interesting property of AChR blockers is that, when bound to the pore, many of them affect the kinetics of interconversion among allosteric states (closed, open, and desensitized), as demonstrated by Neher and Steinbach (1978) for QX compounds. This makes the use of blockers an appealing tool to probe functional aspects of the activation gate and its relationship with the desensitization gate.

In this paper, we studied the channel-blocking properties of choline on the muscle-type AChR. The goal was to understand how choline block affects the kinetics of gating and desensitization because we were interested in obtaining an estimate of the affinity of the receptor's transmitter binding sites for this molecule (see Purohit and Grosman on p. 719 of this issue), and block is prominent at the concentrations of choline used during activation assays. The three main results of our

Correspondence to Claudio Grosman: grosman@life.uiuc.edu

Abbreviations used this paper: AChR, nicotinic acetylcholine receptor channel.

single-channel analysis are as follows. (1) The apparent dissociation equilibrium constant of choline from the AChR's open pore (K_B) is ~12 mM (in the presence of ~155 mM K^+ and Na^+, and 3.5 mM Ca^{2+} and Mg^{2+}). That is, the affinity of the pore for choline is lower than that of the transmitter binding sites ($K_{D,\ Choline} \cong 4.1$ mM; Purohit and Grosman, 2006) by a factor of only ~3. (2) The closing rate constant of choline-diliganded, choline-blocked AChRs is slower than that of choline-diliganded unblocked channels by a factor of ~13 (~300 s^{-1} and ~3,900 s^{-1}, respectively, in the wild-type receptor, and ~65 s^{-1} and ~850 s^{-1} in an M2–M3 linker mutant). (3) And the rate constant of entry into desensitization is the same regardless of whether the pore is blocked by choline or not (32 s^{-1}, in the wild type, and 18 s^{-1}, in the mutant). These results provide all that is needed to correct for the lengthening of (apparent) open intervals caused by choline block, a correction that is necessary to interpret the activation of the AChR with choline as the agonist. Also, the markedly different effect of block on the rate constants of channel closing and channel entry into desensitization supports the notion of the activation and desensitization gates of the muscle AChR acting as distinct molecular entities.

MATERIALS AND METHODS

Adult mouse muscle AChR cDNA clones (Gardner, 1990; Sine, 1993) were provided by S.M. Sine (Mayo Clinic, Rochester, MN) in the CMV-based expression vector pRBG4 (Lee et al., 1991). The αS269I mutation was introduced using the QuikChange Site-directed Mutagenesis Kit (Stratagene). The complete DNA sequences of all inserts were confirmed by dideoxy sequencing. Approximately 24 h before transfection, HEK 293 cells were seeded onto 35-mm plastic culture dishes. The cells were transiently transfected using the calcium-phosphate precipitation method using ~1 μg of total cDNA per 35-mm dish. The transfection was allowed to proceed at 37°C for ~15 h, after which the medium was changed.

Single-channel recordings were performed in the cell-attached configuration (Hamill et al., 1981) at ~22°C, ~24 h after changing the culture medium. Pipette resistances typically ranged between 8 and 10 MΩ. To maximize control on the voltage applied to the patch, a potassium-based bath solution was used. This solution, which was also used in the pipette, contained (in mM) 142 KCl, 5.4 NaCl, 1.8 $CaCl_2$, 1.7 $MgCl_2$, and 10 HEPES/KOH, pH 7.4. In addition, the pipette solution contained choline at the indicated concentrations. Choline chloride was obtained from Sigma-Aldrich and was used without further purification. All other chemicals were obtained from Acros Organics.

Unless otherwise stated, the patch pipette was held at a potential of +100 mV (i.e., the transmembrane potential was −100 mV). Single-channel currents were recorded using an Axopatch 200B amplifier (Molecular Devices), stored in videotape format using a PCM-VCR combination (VR-10B, f_c = 37 kHz; Instrutech Corporation), and digitized at 100 kHz (National Instruments card PCI-MIO-16E-4).

Single-channel traces were analyzed using the QuB suite of programs (www.qub.buffalo.edu) and a set of in-house developed subroutines. Current idealization was performed using the SKM option in QuB (Qin, 2004) at an effective bandwidth of DC-18 kHz. Single-channel current amplitudes (Figs. 3 and 6) were estimated as part of the idealization process.

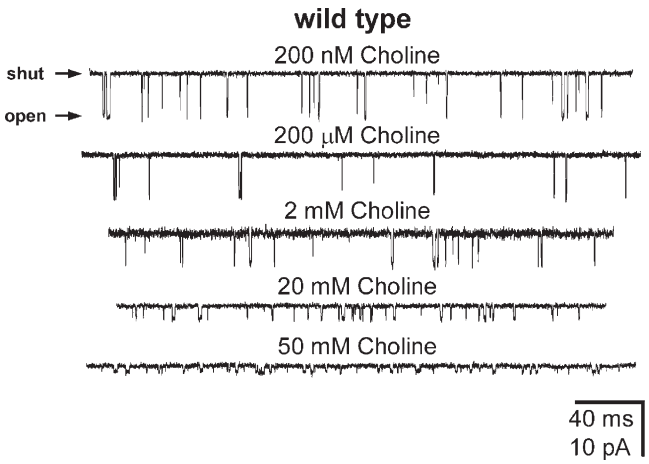

Figure 1. Wild-type AChR single-channel inward currents elicited by various concentrations of choline. Membrane potential ≅ −100 mV. Display $f_c \cong 4$ kHz. Openings are downward deflections. Fast open-channel block by choline is manifest as a concentration-dependent decrease in the single-channel current amplitude and as a prolongation of the (apparent) open times.

The mean durations of $OA_2 \rightleftharpoons OA_2B$ bursts at different choline concentrations (Fig. 4 A and Fig. 7) were estimated as the time constant of the longest-lived component of (apparent) open-time distributions. Because kinetic models cannot be avoided in QuB, the parameters of the corresponding probability density functions were computed from the estimates of transition rates with approximate allowance for missed events (time resolution = 25 μs). In turn, these transition rates were estimated from maximum-likelihood fits to dwell-time series using the MIL option in QuB (Qin et al., 1996). The kinetic schemes used in this step (Purohit and Grosman, 2006) were not ascribed any particular physical meaning; they were simply chosen so as to maximize the likelihood of the parameters, as gauged by the Schwarz criterion (Schwarz, 1978).

Clusters of single-channel currents were identified (Figs. 8–11) using the criterion proposed by Jackson et al. (1983) with only minor modifications (Purohit and Grosman, 2006). The mean durations of intracluster open and shut intervals, as well as the mean number of openings within clusters, were estimated from the duration and number of idealized events. All curve fitting was performed with SigmaPlot software (SPSS), whereas the numerical computation of eigenvalues (Fig. 14) was performed with Maple 6.0 software (Waterloo Maple).

RESULTS

Choline both activates and blocks the muscle AChR (Fig. 1) and, in this respect, it resembles other positively charged agonists of this receptor (Sine and Steinbach, 1984; Ogden and Colquhoun, 1985; Carter and Oswald, 1993, Maconochie and Steinbach, 1995). Like ACh and carbachol, for example, increasing concentrations of choline on the extracellular side reduce the apparent single-channel conductance. This is because the fast kinetics of open-unblocked ⇌ open-blocked "bursts" (Fig. 2) exceed the temporal resolution of typical

patch-clamp recordings. As a result, the observed current level lies somewhere between the zero current and the "true" open-channel current levels, as indicated by Eq. 1. Unlike ACh or carbachol, however, increasing concentrations of choline do not give rise to an excess of detectable short-lived excursions to the zero current level, and the extra open-channel noise is much smaller. These observations suggest that the kinetics of association and dissociation to and from the open-channel pore are particularly fast in the case of choline. The affinity of the open pore for choline and the voltage dependence of block were investigated by recording single-channel current–voltage (I-V) curves (Fig. 3) at different concentrations of choline and at a fixed concentration of K^+ (~150 mM), Na^+ (5.4 mM), Ca^{2+} (1.8 mM), and Mg^{2+} (1.7 mM). Since high concentrations of choline (>100 mM) reduced the current to undetectable levels, the I-V "surface" was globally fitted with an equation of the form:

$$i_B = i_0 \frac{K_B}{K_B + B}, \quad (1)$$

where i_B is the current as a function of both blocker concentration and voltage, i_0 is the current in the absence of blocker, B is the concentration of choline in the patch pipette, and K_B is the (apparent) dissociation equilibrium constant of choline from the open-channel pore. Because the conductance of the unblocked channel is quite constant in the voltage range tested (from −200 to −40 mV), i_0 is expressed as γV, where γ is a constant representing the single-channel conductance of the unblocked AChR, and V is the transmembrane potential. To allow for the voltage dependence of the affinity of the open pore for the blocker, we expressed K_B as $K_{B0}\, e^{0.04\delta V}$ (at 22°C), where K_{B0} is the reciprocal of the open pore's affinity at zero transmembrane potential, δ is the fraction of the transmembrane electric field traversed by a single positive charge moving from the extracellular side to the blocker's binding site, and where the transmembrane potential goes in millivolts. Thus, the fit with Eq. 1 had three unknowns: γ, K_{B0}, and δ. Their fitted values were $\gamma = 75.8 \pm 0.4$ pS, $K_{B0} = 12.5 \pm 1.1$ mM, and $\delta = 0$ (Fig. 3). It may be noted, though, that the expression $K_B = K_{B0} e^{0.04\delta V}$ is based on a permeation model that is physically unrealistic, if only because it ignores the competition between the positively charged choline and the current-carrying cations (mostly K^+ in our case) for a place in the pore, and because it only allows for the dissociation of choline back to the extracellular side of the membrane, even when choline is very likely to permeate the AChR (Dwyer et al., 1980). One can certainly think of more realistic models but these have more free parameters, and our "I-V surface" data do not contain enough information for them to be estimated with confidence. Thus, the K_{B0} value of 12.5 mM should be taken as a "phenomenological" measure of affinity rather than as the equilibrium constant of a well-defined association/dissociation step. Also, the value of zero for the electrical distance ($\delta = 0$) should be taken as an indication that the I-V curves at different concentrations of blocker take the form of straight lines of different slopes (Fig. 3), rather than as an evidence for the binding site of choline inside the pore being isopotential with the extracellular compartment. In conclusion, the results of the fit with Eq. 1 provide an adequate description of the phenomenon of choline block but are not mechanistically illuminating. What is clear from Fig. 3, though, is that block of muscle AChRs by choline is much less voltage dependent than block by ACh. That is, I-V curves recorded in the presence of choline display much less curvature than those recorded in the presence of ACh (Sine and Steinbach, 1984). Most likely, this observation simply reflects a faster permeation rate constant for the smaller choline cation, rather than a shallower depth for the pore-blocking choline binding site.

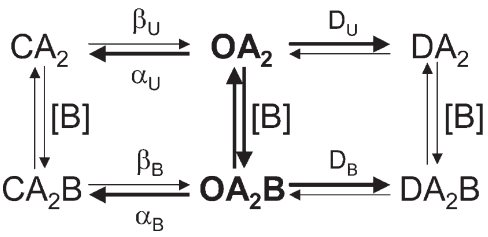

Figure 2. Kinetic scheme used to interpret the effect of choline block on the kinetics of AChR gating and desensitization. For simplicity, this scheme only displays the diliganded receptor. The closed, open, and desensitized states are denoted as C, O, and D, respectively. Choline acting as an agonist is denoted as A. Choline acting as a blocker is denoted as B. The opening, closing, and entry-into-desensitization rate constants of the unblocked (β_U, α_U, D_U) and blocked (β_B, α_B, D_B) forms of the receptor are indicated. The ratio between the blocker dissociation rate constant and the blocker association rate constant gives the blocker dissociation equilibrium constant. In this paper, the dissociation equilibrium constant from the open-channel pore is denoted as K_B, whereas that from the closed-channel pore is denoted as G_B. The reaction steps that dictate the mean duration of choline-diliganded (apparent) openings (Eq. 2) are indicated as bold arrows.

Choline Block and the Prolongation of Apparent Open Intervals

The traces in Fig. 1 show that, as the concentration of blocker increases, not only does the amplitude of single-channel openings decrease, but the duration of (apparent) open intervals also becomes prolonged. This is reminiscent of the effect of the lidocaine derivative QX-222 on this receptor, described by Neher and Steinbach (1978). Fig. 2 shows the kinetic scheme we used to interpret the effect of channel block on gating and desensitization of diliganded receptors (the same scheme would

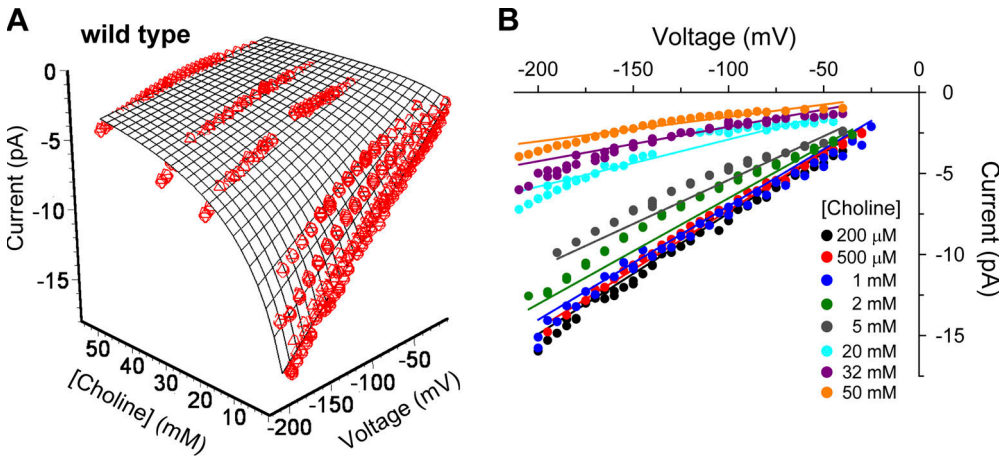

Figure 3. Voltage and concentration dependence of wild-type AChR block by choline. All data points were globally fitted with Eq. 1 assuming that choline can only dissociate back to the extracellular solution, that the voltage dependence of K_B can be expressed as $K_B = K_{B0}e^{0.048\delta V}$, and that the unblocked current (i_0) is a linear function of the transmembrane potential ($i_0 = \gamma V$). The fitted values were: $\gamma = 75.8 \pm 0.4$ pS, $K_{B0} = 12.5 \pm 1.1$ mM, and $\delta = 0$. The estimates of K_{B0} and δ can be regarded largely as phenomenological descriptors of choline block, but they are probably devoid of mechanistic meaning (see Results for a longer discussion). (A) Data displayed as a 3-D plot. (B) Data displayed as separate I-V curves at the indicated concentrations of blocker. Note that the solid lines were calculated using the parameters obtained from the global fit. The limited ability of Eq. 1 to fit the entire dataset, which is particularly evident at 2 and 5 mM choline, most likely reflects the inaccuracies of the permeation model used.

apply for mono- and unliganded AChRs). Because of their decreased current amplitude, and because each choline-diliganded activation of the AChR appears to consist of a single channel opening, these (apparent) open intervals are interpreted as bursts of rapidly alternating sojourns in OA_2 and OA_2B (hence, the term "apparent") that terminate through closing or entry into desensitization of either the unblocked or the blocked channel (Fig. 2). Since the blocking and unblocking transition rates are much faster than the closing and desensitization rate constants, the distribution of diliganded burst times (i.e., the distribution of $OA_2 \rightleftharpoons OA_2B$ burst durations) is very well approximated by a single-component exponential density function, the mean of which is almost exactly given by (Neher and Steinbach, 1978):

$$\text{Mean duration of } OA_2 \rightleftharpoons OA_2B \text{ bursts} = \frac{1}{\frac{K_B}{K_B + B}(\alpha_U + D_U) + \frac{B}{K_B + B}(\alpha_B + D_B)}, \quad (2)$$

where K_B is the dissociation equilibrium constant of choline from the open-channel pore, B is the concentration of choline in the pipette, $(\alpha_U + D_U)$ is the "shutting" rate (i.e., the sum of the closing and entry-into-desensitization rate constants) of unblocked channels, and $(\alpha_B + D_B)$ is the shutting rate of blocked channels (Note that, in this paper, we use the term "shutting rate" to refer to the sum of the closing and entry-into-desensitization rate constants. Other authors use "shutting rate [constant]" to refer to the closing rate constant only). From Eq. 1, $K_B/(K_B + B) = i_B/i_0$, a ratio we call the "fractional current," and which we denote as F in the equations. Thus, Eq. 2 can be rewritten, for simplicity, as:

$$\text{Mean duration of } OA_2 \rightleftharpoons OA_2B \text{ bursts} = \frac{1}{F(\alpha_U + D_U) + (1 - F)(\alpha_B + D_B)}. \quad (3)$$

From these expressions, it follows that if blocked AChRs could neither close nor desensitize (i.e., if $\alpha_B + D_B = 0$), then $OA_2 \rightleftharpoons OA_2B$ bursts would become infinitely long as the extent of channel block increases (i.e., as F approaches zero). Conversely, if the shutting rates were the same, regardless of whether the channel is blocked or not, then the duration of bursts would not change with changes in the extent of block. To estimate the shutting rates of choline-diliganded AChRs with and without choline blocking the pore, we analyzed the distribution of (apparent) open times elicited at a range of choline concentrations (200 nM to 50 mM) that results in a range of fractional-current values between ~0.15 and 1 (Fig. 4 A). The fit with Eq. 3 yielded $(\alpha_U + D_U) = 3{,}941 \pm 240\ s^{-1}$ and $(\alpha_B + D_B) = 329 \pm 72\ s^{-1}$. That is, (apparent) openings get longer as the extent of block increases because open-blocked channels shut more slowly than their unblocked counterparts (by a factor of ~12). With these values, the probability of the channel shutting while still blocked can be calculated, from Fig. 2, as:

$$\text{Probability of a burst terminating from } OA_2B = \frac{(1 - F)(\alpha_B + D_B)}{F(\alpha_U + D_U) + (1 - F)(\alpha_B + D_B)} \quad (4)$$

and the probability of the channel shutting while unblocked, as:

$$\text{Probability of a burst terminating from } OA_2 = \frac{F(\alpha_U + D_U)}{F(\alpha_U + D_U) + (1 - F)(\alpha_B + D_B)}. \quad (5)$$

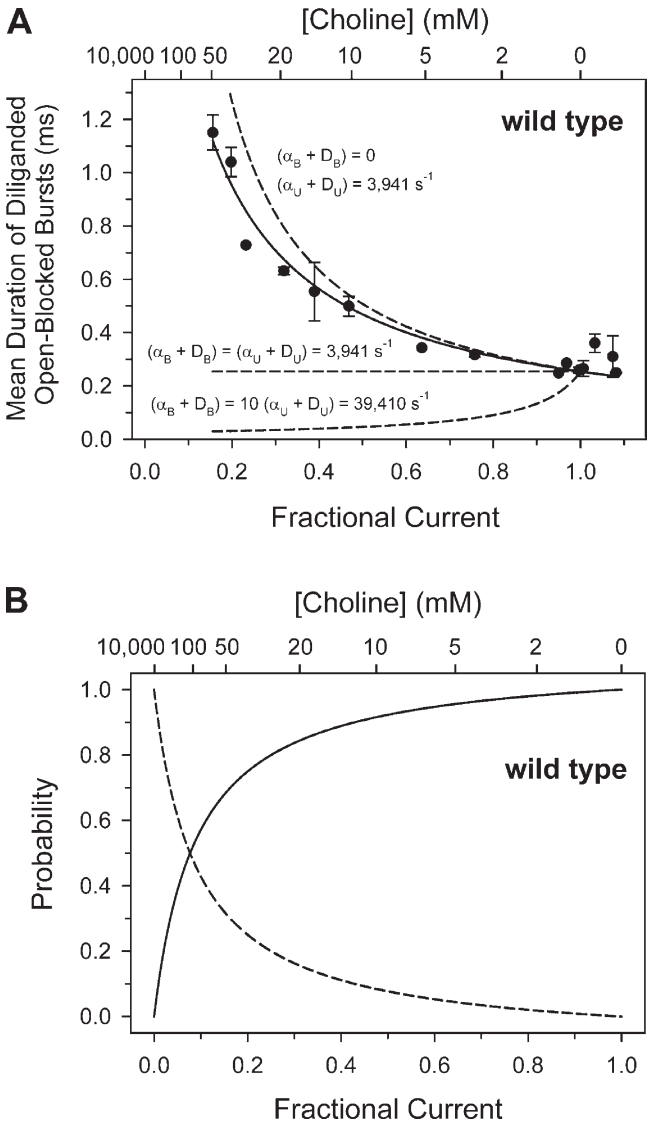

Figure 4. Kinetic properties of wild-type $OA_2 \rightleftharpoons OA_2B$ bursts at −100 mV. (A) The mean durations of choline-diliganded open-blocked bursts, at different choline concentrations, were estimated as indicated in Materials and Methods. Fractional-current values were estimated as the ratio between the observed single-channel current amplitude and −7.58 pA (γ = 75.8 pS, from Fig. 3). Because of the inevitable variation in their estimates, the average single-channel current amplitude at some of the non-blocking concentrations of choline turned out to be somewhat greater than −7.58 pA. This explains why the fractional-current values of some of the points in the plot are larger than unity. Each experimental point corresponds to 1 of 15 different choline concentrations, between 200 nM and 50 mM. The solid line is the fit of the data with Eq. 3. The estimated unblocked channel shutting rate was $(\alpha_U + D_U) = 3{,}941 \pm 240\ s^{-1}$. The estimated blocked channel shutting rate was $(\alpha_B + D_B) = 329 \pm 72\ s^{-1}$. The dashed line plots show three hypothetical different scenarios. In all of them, the unblocked channel shutting rate is assumed to be the same ($\alpha_U + D_U = 3{,}941\ s^{-1}$), whereas the shutting rate of the blocked channel is assumed to be either infinitely slow, equal to that of the unblocked channel, or even faster. The predictions of these three plots are very different from one another and from the experimental observations. To facilitate the interpretation of this figure, the top x axis contains the choline concentration scale. Vertical error bars are standard errors. (B) The probability of an $OA_2 \rightleftharpoons OA_2B$ burst shutting (i.e., closing or entering a desensitized state) from OA_2 is shown as a solid line plot (Eq. 5), whereas the probability of shutting from OA_2B is shown as a dashed line (Eq. 4). The shutting rates estimated in A were used for computing these probabilities.

Fig. 4 B shows these probabilities for the choline-diliganded wild-type AChR, as a function of the fractional current.

The Case of the αS269I Mutant

To confirm the notion that the presence of choline as a blocker slows down channel shutting by a factor of ∼12, we recorded single-channel currents from the M2–M3 linker mutant αS269I (Fig. 5; Croxen et al., 1997; Zhou et al., 1999). This mutant provides a good test case for this hypothesis because the gating rate constants of αS269I AChRs are quite different from those of the wild type (closing is slower by a factor of ∼4.6 [Figs. 7 and 9], and opening is faster by a factor of ∼16 [Fig. 11]), and because the mutation, located in the extracellular M2–M3 linker, is unlikely to affect choline block directly. As a first step, we estimated the affinity of this mutant's open pore for choline. To this end, we plotted the fractional current ($i_B/i_o = K_B/(K_B + B)$) at −100 mV as a function of the concentration of choline (Fig. 6). The fit yielded $K_B = 10.4 \pm 1.3$ mM, a value that is reassuringly close to the wild type's (∼12.5 mM).

Next, we analyzed the distribution of (apparent) open times following the same procedures as for the wild type. The concentration of choline in our recordings ranged from 200 μM to 50 mM, which resulted in a range of fractional-current values between ∼0.17 and 1 (Fig. 7). The fit with Eq. 3 yielded $(\alpha_U + D_U) = 873 \pm 53\ s^{-1}$ and $(\alpha_B + D_B) = 82 \pm 17\ s^{-1}$. Thus, the ratio of shutting rates is ∼11, in good agreement with the effect of choline block on shutting in the case of wild-type receptors.

A Correction for the Block-induced Prolongation of Apparent Openings

Because the affinity of the closed-state AChR's transmitter binding sites for choline ($K_{D,\,Choline} \cong 4.1$ mM; Purohit and Grosman, 2006) is not very different from the affinity of the open-channel's pore ($K_{B,\,Choline} \cong 12.5$ mM; Fig. 3), open-channel block is prominent during activation assays. As shown in Fig. 4 A, channel block distorts the duration of observed openings, and this "artifact" needs to be corrected if we want to understand how choline binds to and gates the AChR. To this end, we define a "prolongation factor" as the extent to which a true opening is prolonged when blocker is present in the solution:

$$\text{Prolongation factor} = \frac{\text{Mean burst duration}}{\text{True-opening duration}} = \frac{(\alpha_U + D_U)}{F(\alpha_U + D_U) + (1-F)(\alpha_B + D_B)} \quad (6)$$

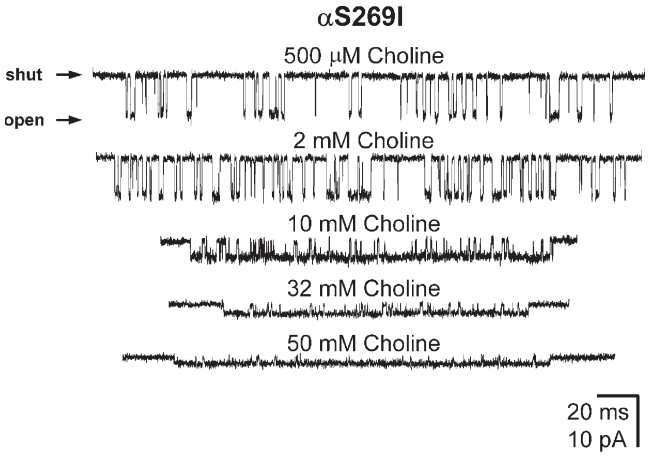

Figure 5. αS269I AChR single-channel inward currents elicited by various concentrations of choline. Membrane potential ≅ −100 mV. Display f_c ≅ 4 kHz. Openings are downwards.

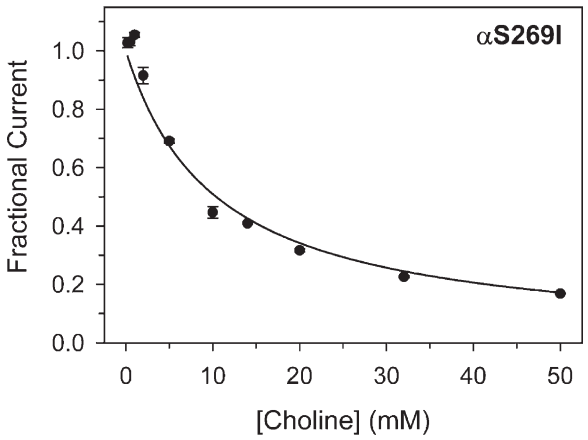

Figure 6. Affinity of the αS269I mutant open-channel pore for choline. All measurements were done at −100 mV. The data were fitted with the following: Fractional current = $K_B/(K_B + B)$. The estimated value of K_B was 10.4 ± 1.3 mM, quite close to the wild-type estimate of ∼12.5 mM. Vertical error bars are standard errors.

and, rearranging, we have:

$$\text{Prolongation factor} = \frac{1}{F + (1-F)\dfrac{(\alpha_B + D_B)}{(\alpha_U + D_U)}}, \quad (7)$$

where the $(\alpha_B + D_B)/(\alpha_U + D_U)$ ratio (i.e., the ratio of shutting rates) is a constant for choline (∼1/12; Fig. 4 A and Fig. 7). Therefore, experimentally obtained open durations can be corrected using Eq. 7, by dividing the observed mean burst duration by the prolongation factor that corresponds to the particular degree of block (i.e., the "F" term). We applied this correction to data recorded from the AChR activated by mixtures of ACh and choline in which only choline was present at concentrations that were high enough to prolong (apparent) openings (Purohit and Grosman, 2006). This correction is based on the reasonable assumption that the extent of prolongation is the same as long as choline is the only blocking agent. That is, the same prolongation factor applies regardless of whether the transmitter binding sites are unliganded, ACh or choline monoliganded, ACh or choline diliganded, or heterodiliganded. For reasons of experimental design, however, it was most convenient to determine this factor on choline-diliganded channels (Fig. 4 A).

Desensitization

Although the ratio of unblocked-to-blocked shutting rates provides all that is needed to correct for the prolongation of (apparent) openings, it would be desirable, from a point of view of mechanisms, to estimate the effect of choline block on closing and desensitization separately. It can be shown that the total time a channel spends in the open state (oscillating between OA_2 and OA_2B) within a cluster of single-channel diliganded openings depends on the entry-into-desensitization rate constants of the unblocked (D_U) and blocked (D_B) channels but not on the closing rate constants (α_U and α_B):

$$\text{Mean total open time within clusters} = \frac{1}{FD_U + (1-F)D_B}. \quad (8)$$

A "cluster" (Sakmann et al., 1980) is defined as a set of state transitions that starts when a desensitized channel opens and ends when the channel, after a number of closings and reopenings, enters a desensitized state again. In other words, a cluster consists of a series of visits to open and closed states flanked by sojourns in desensitized states. Identification of such clusters is not trivial, but it is a common practice in single-channel analysis. Following the procedures elaborated in Purohit and Grosman (2006), we identified clusters of wild-type single-channel openings in recordings obtained at choline concentrations between 14 and 50 mM, resulting in a range of fractional-current values between ∼0.15 and ∼0.4 (Fig. 8). The narrower range of choline concentrations is due to the fact that the lowest concentration of choline that allowed us to identify clusters of wild-type AChR openings with confidence was 14 mM. Above 50 mM, on the other hand, the current amplitude is too small to be detected unambiguously. The mean total open time within these clusters (i.e., the y axis values in Fig. 8) was calculated as the product of the mean duration of intracluster open-blocked bursts and the mean number of such bursts in a cluster. However, since only clusters with five or more openings were selected for this analysis (this threshold is often necessary to eliminate openings of dubious origin), the observed mean number of bursts per cluster is an overestimate of the true mean. Assuming that, under the equilibrium

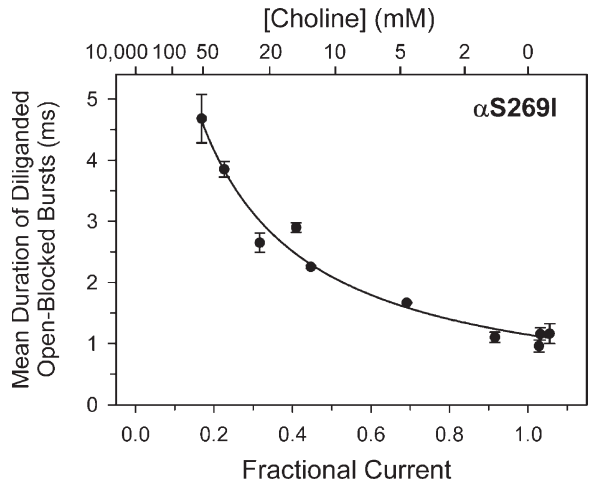

Figure 7. Kinetic properties of αS269I $OA_2 \rightleftharpoons OA_2B$ bursts at −100 mV. The mean durations of choline-diliganded open-blocked bursts were estimated as in Fig. 4 A, for the wild type. Each experimental point corresponds to 1 of 10 different choline concentrations, between 200 μM and 50 mM. The solid line is the fit of the data with Eq. 3. The estimated unblocked-channel shutting rate was $(\alpha_U + D_U) = 873 \pm 53\ s^{-1}$. The estimated blocked-channel shutting rate was $(\alpha_B + D_B) = 82 \pm 17\ s^{-1}$. Note that, even though these two shutting rates are quite different from their wild-type counterparts, the unblocked-to-blocked ratios are very similar (∼11 in the mutant, ∼12 in the wild type). The top x axis contains the choline concentration scale. Vertical error bars are standard errors.

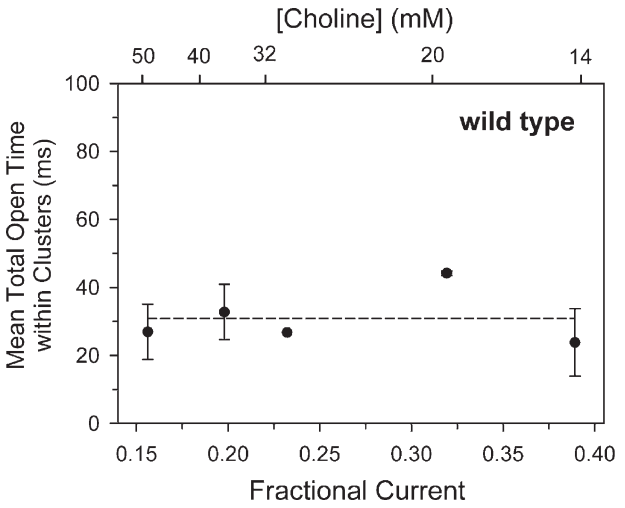

Figure 8. Effect of choline block on the wild-type rate constant of entry into desensitization. The mean total open time within clusters (Eq. 8) turned out to be rather insensitive to the fractional current. This suggests that the operation of the desensitized gate, at least in the entry-into-desensitization direction, is largely unaffected by choline block. The average of the mean total open time within clusters across choline concentrations (horizontal dashed line) is 31 ± 4 ms. Thus, in the wild type, $D_U \cong D_B \cong 32\ s^{-1}$ (see Fig. 2). Vertical error bars are standard errors.

conditions of our experiments, desensitized states are connected to open and closed states through the diliganded open state (i.e, OA_2 or OA_2B), the number of openings within a cluster is a one-component, geometrically distributed random variable, the mean of which is given by:

$$\text{Mean} = \sum_{k=1}^{\infty} kq(1-q)^{k-1} = \frac{1}{q}, \tag{9}$$

where k is the number of openings in a cluster ($k = 1 \ldots \infty$), and q is the probability of the open-diliganded channel (either unblocked or blocked) entering a desensitized state rather than closing. But if the distribution is truncated (as in our case), so that only clusters containing "m" or more openings are considered, then the computed mean is larger than the true mean:

$$\text{Mean of the truncated distribution} = \sum_{k=m}^{\infty} kq(1-q)^{k-m} = \frac{1}{q} + m - 1. \tag{10}$$

Hence, for each patch, the mean number of openings within clusters was estimated by subtracting (m – 1) from the observed mean.

The values of total open time within clusters, so calculated, appear to be quite insensitive to the extent of block (Fig. 8), which strongly suggests that the rate constant of entry into desensitization is the same regardless of whether the open channel is blocked or not. The average across different choline concentrations is 31 ± 4 ms and, thus, $D_U \cong D_B \cong (31\ ms)^{-1} = 32\ s^{-1}$. From this value, and the unblocked and blocked shutting rates, it follows that $\alpha_U \cong (3{,}941 - 32)\ s^{-1} \cong 3{,}909\ s^{-1}$ and $\alpha_B \cong (329 - 32)\ s^{-1} \cong 297\ s^{-1}$. The ratio of closing rate constants is ∼13.

If the analysis above were correct, then the effect of choline block on the kinetics of channel closing would be very different from its effect on the kinetics of entry into desensitization. However, the large patch-to-patch variation in the estimates of the mean total open time within clusters (see the vertical error bars in Fig. 8), and the narrow range of choline concentrations that could be tested on the wild type, may cast some doubts on these results. With respect to the large patch-to-patch variation, it should be noted that the time constant of the macroscopic current decay that occurs during application of ACh (which, at least in the wild type, is a good approximation to the reciprocal of the rate constant of entry into desensitization) also shows a large scatter. Dudel and coworkers (Franke et al., 1993) reported values as fast as 10 ms and as slow as 61 ms for the embryonic-type AChR upon application of 100 μM ACh for 200–300 ms to fast-perfused outside-out patches. Similarly, unpublished estimates of the desensitization time constant from our own laboratory (100 μM ACh, 2-s applications to fast-perfused outside-out patches) range from ∼21 to ∼59 ms in the adult-type

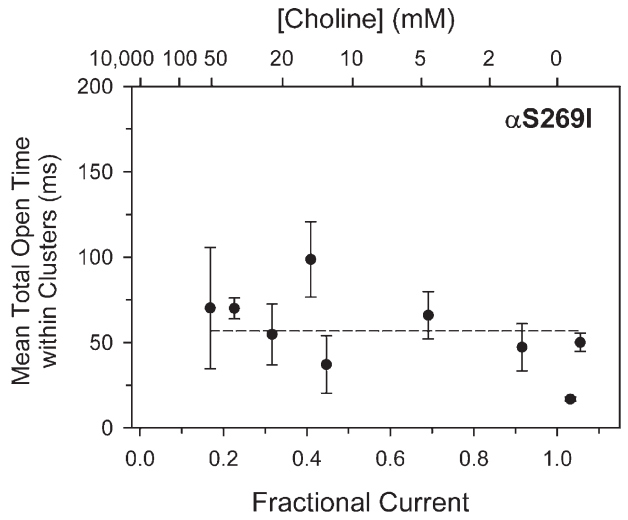

Figure 9. Effect of choline block on the αS269I mutant rate constant of entry into desensitization. This rate constant was estimated as in Fig. 8, for the wild type. A wider range of choline concentrations could be tested on this mutant because lower concentrations of the ligand were needed to start detecting clear clusters of single-channel openings. As was the case for the wild type, the mean total open time within clusters (Eq. 8) proved to be insensitive to the fractional current. The average of the mean total open time within clusters across choline concentrations (horizontal dashed line) is 57 ± 8 ms. Thus, in the αS269I mutant, $D_U \cong D_B \cong 18\ s^{-1}$ (see Fig. 2). Vertical error bars are standard errors.

(eight patches) and from ~23 to ~96 ms in the embryonic-type receptor (three patches). It appears, then, that the large variability of desensitization rate constants is typical of the AChR, and that it cannot be attributed completely to limitations of the methods used here to identify clusters of single-channel openings. On the other hand, to address the issue of the narrow range of choline concentrations, we repeated the same type of analysis shown in Fig. 8 to currents recorded from the αS269I mutant. Because of the faster choline-diliganded opening rate constant of this mutant (a factor of ~16 with respect to the wild type; see Figs. 10 and 11), identifiable clusters could be elicited at concentrations of choline as low as 500 μM and, so, the range of choline concentrations that could be tested was much wider (Fig. 9). Again, as was the case for the wild type, the kinetics of entry into desensitization do not seem to be affected by choline block. The average of the mean total open time values across choline concentrations is 57 ± 8 ms and, thus, $D_U \cong D_B \cong (57\ ms)^{-1} = 18\ s^{-1}$. From this value, and the unblocked and blocked shutting rates, it follows that $\alpha_U \cong (873 - 18)\ s^{-1} \cong 855\ s^{-1}$ and $\alpha_B \cong (82 - 18)\ s^{-1} \cong 64\ s^{-1}$. That is, the ratio of unblocked-to-blocked closing rate constants is ~13 for the αS269I mutant, the same number as for the wild type (see above).

The fact that the kinetics of entry into desensitization are not affected by choline block would hint that the blocker does not interfere with the operation of the desensitization gate. However, the reverse reaction, namely recovery from desensitization under equilibrium conditions, needs to be studied as well before drawing a firm conclusion in this respect. Information on the kinetics of recovery is provided by the distribution of durations of shut intervals between successive clusters of single-channel openings arising from the same channel. But, since under our experimental conditions membrane patches contain an unknown number of AChRs, the exact time it takes for any given desensitized channel to reopen cannot be estimated from the observed durations of intercluster intervals; this is because any two consecutive clusters in a recording may arise from different channels. Despite this difficulty, however, large changes in the kinetics of recovery from desensitization are expected to be evident in cell-attached recordings if the differences in the number of channels among patches are comparatively small. Examination of the shut-time distributions corresponding to recordings obtained at different concentrations of choline failed to reveal such large changes in the distribution of intercluster intervals. A more complete study, one that includes the estimation of the number of channels present in each patch, is clearly needed.

The Opening Rate Constants of the Unblocked and Blocked Channel

Eqs. 4 and 5 give the probability of an $OA_2 \rightleftharpoons OA_2B$ burst ending (i.e., shutting) from either the blocked or the unblocked open-diliganded states. Similarly, the probabilities of the open channel closing from either OA_2B or OA_2 are given by:

$$\text{Probability of the channel closing from } OA_2B = \frac{(1-F)\alpha_B}{F\alpha_U + (1-F)\alpha_B} \tag{11}$$

and

$$\text{Probability of the channel closing from } OA_2 = \frac{F\alpha_U}{F\alpha_U + (1-F)\alpha_B}. \tag{12}$$

Since, at least in the wild type, closing is much faster than desensitization ($\alpha_U > D_U$ and $\alpha_B > D_B$), a plot of these probabilities as a function of F would not be very different from the plot in Fig. 4 B for the shutting (i.e, closing plus desensitization) probabilities. The closing probabilities in Eqs. 11 and 12 are relevant because, due to the detailed-balance constraint (Fig. 2), the probability of the AChR closing while blocked by choline (Eq. 11) is equal to the probability of the channel opening from CA_2B. Similarly, the probability of the channel closing while unblocked (Eq. 12) is equal to the probability of the channel opening from CA_2. Thus, using the

estimated K_B (~12.5 mM) and the ratio of closing rate constants (~13), we can calculate that at 20 mM choline, for example, ~10% of all diliganded openings proceed from CA_2B to OA_2B, rather than from CA_2 to OA_2. And at 50 mM choline, this fraction rises to ~25%. This reminds us that, in the same way as the observed shutting rate (i.e., the reciprocal of Eq. 3) is actually a mixture of a blocked and an unblocked channel shutting rate, the observed opening rate (which we estimate as the reciprocal of the mean duration of intracluster shut intervals measured at concentrations of choline that saturate the transmitter binding sites) could also be a mixture of two opening rate constants. From Fig. 2, and assuming that the kinetics of block and unblock to and from the closed channel are much faster than the opening rate constants β_U and β_B, it can be shown that the distribution of intracluster shut intervals, measured at saturating choline concentrations, is very well approximated by a single-component exponential density function. Its mean is given by:

$$\text{Mean duration of } CA_2 \rightleftharpoons CA_2B \text{ bursts} = \frac{1}{\frac{G_B}{G_B+B}\beta_U + \frac{B}{G_B+B}\beta_B}, \quad (13)$$

where G_B is the (apparent) dissociation equilibrium constant of choline from the closed-channel pore, B is the concentration of choline in the pipette, and $B/(G_B + B)$ is the probability of the closed channel being blocked. The possibility that the duration of choline-diliganded intracluster shut intervals reflects anything other than just the unblocked-channel opening rate constant (β_U) is of fundamental importance because, when it comes to elucidate activation mechanisms (Grosman and Auerbach, 2000; Purohit and Grosman, 2006) or to probe general aspects of the chemical dynamics of the gating conformational change using choline as the agonist (e.g., the transition-state structure; Grosman et al., 2000), we are only interested in the opening (and closing) rate constant of the unblocked receptor; in those cases, we do not care about the gating properties of the blocked AChR. So what exactly are we measuring with the reciprocal of these (monoexponentially distributed) intracluster shut times? β_U? β_B? A combination of the two? Of course, it would be very helpful to have the $CA_2 \rightleftharpoons CA_2B$ counterpart of plots like those in Fig. 4 A and Fig. 7, and to be able to fit such data with the closed-state version of Eq. 3 to estimate the two opening rate constants (blocked and unblocked) unequivocally. But, obviously, there is no way of estimating the extent of closed-channel block directly using electrophysiological methods, so a precise analysis of the kinetics of $CA_2 \rightleftharpoons CA_2B$ bursts cannot be made. Nevertheless, some qualitative observations are worth elaborating.

Eq. 13 predicts that the observed diliganded opening rate (i.e., the reciprocal of the mean duration of $CA_2 \rightleftharpoons CA_2B$ bursts) is a function of the concentration of blocker. In the absence of block (i.e., when $G_B/(G_B + B) = 1$), the observed opening rate becomes equal to the unblocked opening rate constant (β_U). As the concentration of blocker increases, and the probability of the closed channel being blocked approaches unity, the observed opening rate approaches the opening rate constant of the blocked channel (β_B). In spite of the high patch-to-patch variability, the mean duration of intracluster shut intervals plotted in Fig. 10 is rather insensitive to the concentration of blocker. To make sure that this was indeed the case, we resorted, again, to the αS269I mutant (Fig. 11). The initial shortening of intracluster shut intervals in Fig. 11 is, undoubtedly, due to the transmitter binding sites becoming increasingly occupied with choline but, between 14 and 50 mM, the mean duration of intracluster shut times remains quite constant at ~0.5 ms.

To test whether the data in Figs. 10 and 11 can provide us with clues as to what exactly we are measuring with the intracluster shut-interval durations, we plotted Eq. 13 for a number of possible situations. Assuming an arbitrary value of 125 s^{-1} for β_U, expressing β_B in terms of all other parameters in the cyclic scheme of Fig. 2 (i.e., $\beta_B = \beta_U G_B \alpha_B / K_B \alpha_U$, from detailed balance), and remembering that $K_B \cong 12.5$ mM and $\alpha_U/\alpha_B \cong 13$, Fig. 12 shows Eq. 13 as a function of the concentration of blocker for different G_B values.

Two concepts emerge from a comparison of Fig. 12 with the near constant shut durations plotted in Figs. 10 and 11. One is that the affinity of the closed-channel pore for choline seems to be much lower than that of the open-channel pore (i.e., $G_B/K_B > 1$). Indeed, it can be calculated (Eq. 13) that if $G_B/K_B = 10$, for example, then the mean duration of intracluster shut intervals would have increased by a factor of only ~1.05 as the choline concentration increased from 14 to 50 mM. And if $G_B/K_B = 1{,}000$, this mean duration would have decreased by a factor of ~0.83, probably too small a change to be detected with confidence in our experiments, considering the typical variation among patches. Conversely, the mean duration of intracluster shut intervals would have increased by a factor of ~2, if $G_B/K_B = 1$, by a factor of ~2.8, if $G_B/K_B = 0.1$, or by a factor of ~3, if $G_B/K_B = 10^{-3}$, in going from 14 to 50 mM choline. Such large increases in the observed mean durations would have been easily detected in our experiments. It should be noted that all the calculations above are independent of the particular value of β_U assumed (here, 125 s^{-1}). The calculated factors between 14 and 50 mM are only a function of the α_U/α_B ratio, the K_B value, and the G_B/K_B ratio.

That the G_B/K_B ratio is larger than unity implies (from detailed balance) that the gating equilibrium

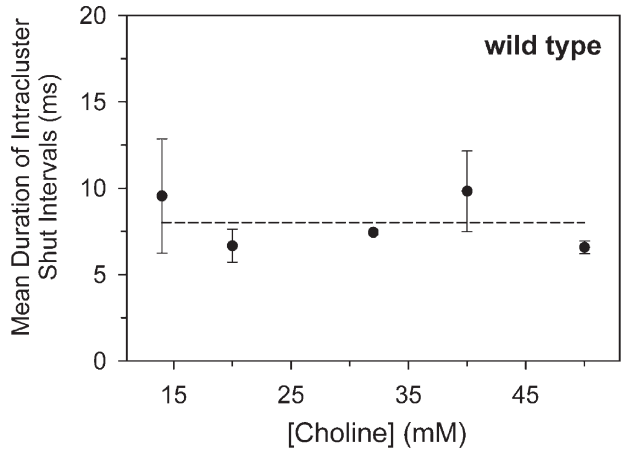

Figure 10. The opening rate constant of choline-diliganded wild-type AChRs. The mean duration of intracluster shut intervals was measured between 14 and 50 mM choline. The average value across choline concentrations (horizontal dashed line) is 8.0 ± 0.7 ms. Vertical error bars are standard errors.

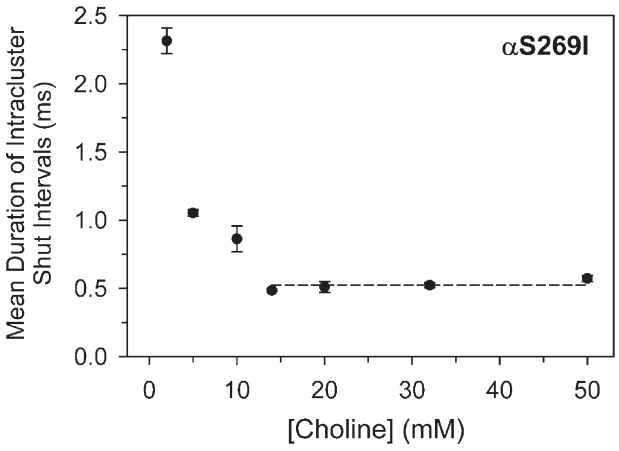

Figure 11. The opening rate constant of choline-diliganded αS269I AChRs. After the initial shortening of intracluster shut intervals, owing to the increasing occupation of the transmitter binding sites, the mean duration of $CA_2 \rightleftharpoons CA_2B$ bursts remains insensitive to the concentration of choline. The average closed-burst duration in the 14–50 mM choline range (horizontal dashed line) is 0.52 ± 0.02 ms. Vertical error bars are standard errors.

constant of the blocked AChR is larger than that of the unblocked channel and, thus, that $\beta_B > \beta_U/13$ (because $\alpha_B \cong \alpha_U/13$). The idea of a faster opening rate constant for the blocked channel, not only faster than $\beta_U/13$ but faster than β_U, seems to be physically realistic; if a perturbation, here channel block, slows down the $OA_2B \rightarrow CA_2B$ rate constant, then it is very likely that the same perturbation also speeds up the reverse, $CA_2B \rightarrow OA_2B$ rate constant. This follows directly from the concept of linear free energy relationships (LFERs; Leffler and Grunwald, 1963), according to which the sensitivity of a transition state's free energy to perturbation is intermediate between the sensitivities of the flanking end states. LFERs have been shown to hold for the $CA_2 \rightleftharpoons OA_2$ reaction of the AChR, at least when perturbed using mutations, different agonists, and different transmembrane potentials (Grosman et al., 2000).

The other notion that arises from Fig. 12 is that, for G_B/K_B values larger than a factor of ~10, the predicted mean duration of choline-diliganded closed sojourns at blocker concentrations between 14 and 50 mM is reassuringly close to the value of this variable in the absence of block (i.e., at B = 0). Thus, the reciprocal of the mean duration of intracluster shut intervals, measured in this range of choline concentrations, seems to be an accurate estimator of the opening rate constant of the (unblocked) choline-diliganded AChR. In the wild type, the average value of the mean duration across choline concentrations is ~8.0 ms (Fig. 10) and, hence, we suggest that $\beta_U \cong 125\ s^{-1}$. In the αS269I mutant, the average value of the mean duration in the 14–50 mM choline range is ~0.5 ms (Fig. 11) and, hence, $\beta_U \cong 2{,}000\ s^{-1}$. The values of the corresponding blocked-channel opening rate constants (i.e., $\beta_B = \beta_U G_B \alpha_B / K_B \alpha_U$) cannot be calculated, however, because the affinity of the closed-channel pore for choline ($1/G_B$) is not known; we only know that G_B is likely to be much larger than K_B.

On the other extreme, if the $CA_2 \rightleftharpoons CA_2B$ interconversion were exceedingly slow (as if the activation gate in its closed position hindered the access of the blocker to and from the pore-blocking site), then an additional closed-time component should have appeared in the intracluster shut-time distribution as the probability of the channel opening from CA_2B (Eq. 11) increased. The time constants of the two components of this distribution would be, simply, $1/\beta_U$ and $1/\beta_B$. Because such an additional component was not evident in our data, we conclude that either the $CA_2 \rightleftharpoons CA_2B$ interconversion is, indeed, very slow and $\beta_B \cong \beta_U$ or the $CA_2 \rightleftharpoons CA_2B$ interconversion is so fast that the distribution of intracluster shut times shows only a single exponential component.

DISCUSSION

Taken together, the experimental data presented here are consistent with choline being a slowly permeating cation of the AChR. The permeation rate must be slow enough not to give rise to measurable choline-carried single-channel currents, yet fast enough to nearly eliminate the curvature of the I-V curves that would result from the voltage-dependent binding and unbinding of charged impermeant blockers to and from the channel pore (Fig. 3). Hence, it is tempting to propose that the pore-blocking site for choline is the selectivity filter itself, and that the (unresolved) blocked intervals result from the longer mean residence time of the choline cation at this site. Moreover, occupancy of the pore-blocking site by choline appears to hinder the operation of the activation gate, slowing its closure down by a factor

of ~13, whereas the desensitization gate seems to remain unaffected, at least in the entry-into-desensitization direction.

However, before we can continue elaborating on the ability of choline block to dissect the activation and desensitization gates, one more question is in order. Is the kinetic scheme in Fig. 2 general enough? Is the mere fact that channel block is accompanied by the prolongation of (apparent) openings enough to conclude that the former causes the latter? Channel closing and entry into desensitization are not the only two possible pathways out of an $OA_2 \rightleftharpoons OA_2B$ burst, so the scheme in Fig. 2 is, certainly, a simplification. As shown in the more general kinetic scheme of Fig. 13, ligand dissociation from the open-state transmitter binding sites provides another route for burst termination (e.g., $OA_2 \rightarrow OA \rightarrow O \rightarrow C$), as suggested for ACh-diliganded receptors (Grosman and Auerbach, 2001). In the case of ACh-liganded wild-type AChRs, the contribution of this third pathway to the termination of a diliganded activation is minimal because the dissociation rate of ACh from OA_2 is relatively slow ($<24\ s^{-1}$; Grosman and Auerbach, 2001). However, the dissociation of choline from the open-state transmitter binding sites could well be much faster because the affinity of the open state for choline is expected to be lower than that for ACh by a factor of ~1,000 (Purohit and Grosman, 2006).

Our data indicates that (apparent) openings get longer as the concentration of blocker increases (Fig. 4 A), a phenomenon we attributed to choline hindering the operation of the activation gate when bound to its pore-blocking site. With this model in mind (Eq. 3), we suggested that unblocked AChRs shut at a rate of ~3,941 s^{-1}, and that this rate drops to ~329 s^{-1} in choline-blocked AChRs. But, how about the dissociation of choline from the transmitter binding sites of OA_2 or OA_2B? At very low concentrations of choline, the contribution of this pathway to the termination of a burst is expected to be maximal because, once a molecule of choline dissociates from the transmitter binding sites ($OA_2 \rightarrow OA$), rebinding is so slow that channel closure inevitably follows ($OA \rightarrow O \rightarrow C$ or $OA \rightarrow CA$). At high concentrations of choline, on the other hand, the contribution of agonist dissociation is expected to be minimal because binding is so fast that dissociation ($OA_2 \rightarrow OA$) is rapidly followed by reassociation ($OA \rightarrow OA_2$). Thus, this scenario also predicts that the mean duration of channel openings increases with increasing concentrations of choline, but the mechanism is fundamentally different and does not involve any interference with the operation of the activation gate at all.

If we recognize that it is possible for choline to dissociate from the open-state transmitter binding sites (and to associate to them), then we can no longer classify openings as arising from diliganded, monoliganded, or unliganded receptors because the number of bound

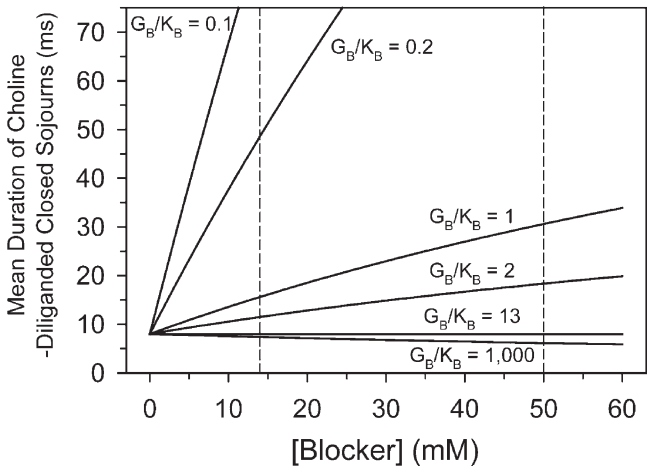

Figure 12. Mean duration of sojourns in the CA_2/CA_2B set of diliganded closed states as a function of blocker concentration. Eq. 13 is plotted for different G_B values assuming that the opening rate constant of the choline-diliganded unblocked AChR (β_U) is 125 s^{-1}. As the concentration of blocker increases, the mean duration of closed-diliganded intervals is expected to approach, asymptotically, the reciprocal of the blocked-channel opening rate constant (i.e., $\beta_B = \beta_U G_B \alpha_B / K_B \alpha_U$, from detailed balance). If $G_B/K_B = 13$, then $\beta_B = \beta_U$, and the mean duration of closed-diliganded sojourns becomes independent of the concentration of blocker.

choline molecules can change during an open period. However, we can still classify openings according to their mean duration. Assuming that the kinetics of gating, desensitization, and agonist binding/unbinding are the same regardless of whether the pore is blocked by choline or not, it can be shown that, at infinitely low concentrations of choline (or any other agonist that elicits single-opening activations, for that matter), the time constant of the slowest component of the open-time distribution is very well approximated by an extremely simple expression:

$$\lim_{[\text{agonist}]\to 0} (\text{slowest open-time constant}) \cong \frac{1}{\alpha + D + 2j}, \quad (14)$$

where α and D are the closing and entry-into-desensitization rate constants of diliganded receptors, respectively, and 2j is the dissociation rate of the agonist from the transmitter binding sites of the diliganded open state (note that the 2j term is all that is needed to capture the effect of agonist dissociation from the open state even though the $OA_2 \rightarrow OA$ transition itself does not terminate an opening). The contribution of agonist dissociation to the termination of an opening decreases, however, as the concentration of agonist increases. As a result, the slowest component of the open-time distribution would become longer and, at infinitely high concentrations, its time constant is given by:

$$\lim_{[\text{agonist}]\to \infty} (\text{slowest open-time constant}) = \frac{1}{\alpha + D}. \quad (15)$$

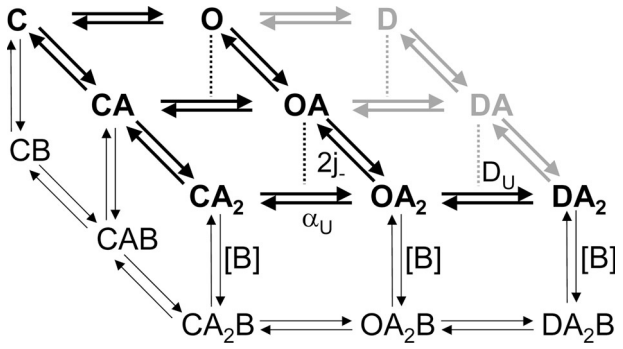

Figure 13. An MWC-type of kinetic scheme (Monod et al., 1965) that includes blocking and unblocking steps. This kinetic model was used to test the hypothesis that the prolongation of (apparent) open times with increasing choline concentrations is due to the increasing rebinding of choline to the transmitter binding sites in the open state (Eqs. 14 and 15), rather than to a more local effect of choline obstructing the closure of the activation gate. To this end, the expected time constant value of the slowest component of the open-time distribution, at each choline concentration, was computed numerically as the reciprocal of the smallest eigenvalue of the open-state submatrix of $-Q$ ($-Q_{oo}$). Since choline block was assumed not to affect the kinetics of gating, desensitization or choline binding/unbinding to/from the transmitter binding sites, only one of the two stacked MWC schemes needed to be considered (say, the one with bold symbols). The model was further simplified by making the plausible assumption that desensitization of open-unliganded and open-monoliganded AChRs is negligible (bold gray symbols). Thus, the kinetic scheme used for the computation of eigenvalues ended up being the one shown with bold black symbols, which further assumes that both transmitter binding sites are functionally equivalent and independent. Since choline-elicited activations consist largely of single openings (unlike ACh-elicited activations, for example), the Q_{oo} partition only includes states OA_2, OA, and O. The values of the rate constants used for the calculations were as follows. Choline-diliganded closing rate constant = 297 s^{-1} (a putative value derived from Fig. 4 A and Fig. 8); choline-diliganded opening rate constant = 125 s^{-1} (from Figs. 10 and 12); unliganded closing rate constant = 12,000 s^{-1} (Grosman, 2003); unliganded opening rate constant = 1.2×10^{-3} s^{-1} (from the arbitrary, but reasonable, assumption that the unliganded gating equilibrium constant is 10^{-7}); choline-monoliganded closing rate constant = 8,500 s^{-1} (a reasonable value, intermediate between its diliganded and unliganded counterparts); choline-monoliganded opening rate constant = 1.75 s^{-1} (from detailed balance); choline-association rate constant to each closed-state transmitter binding site = 100 μM^{-1} s^{-1} (reasonable assumption); choline-dissociation rate constant from each closed-state transmitter binding site = 4.10^5 s^{-1} (from the K_D value of 4.1 mM in Purohit and Grosman, 2006); choline dissociation rate constant from each open-state transmitter binding site = 1,806 s^{-1} (from the putative value of 3,612 s^{-1} for the dissociation rate of choline from the diliganded open state, as discussed in Discussion); choline association rate constant to each open-state transmitter binding site = 895 $\mu M^{-1}s^{-1}$ (from detailed balance); entry-into-desensitization rate constant = 32 s^{-1} (from Fig. 8); recovery-from-desensitization rate constant = 0.01 s^{-1} (reasonable assumption). The reciprocal of the computed eigenvalues are shown in Fig. 14.

Our estimates of shutting rates were 3,941 s^{-1} and 329 s^{-1} at infinitely low and infinitely high choline concentrations, respectively. Could it, then, be that that choline dissociates from the open-diliganded state at a rate of ~3,600 s^{-1} ($2j = 3{,}941\ s^{-1} - 329\ s^{-1} = 3{,}612\ s^{-1}$), and that the observed prolongation of openings is due to the differences between Eqs. 14 and 15, rather than to a local effect of choline on a channel gate? Indeed, if the sum of the closing and entry-into-desensitization rate constants of choline-diliganded AChRs were ~329 s^{-1}, if choline dissociated from the open-diliganded transmitter binding sites at a rate of ~3,600 s^{-1}, and if the kinetics of gating, entry into desensitization, and agonist association/dissociation were completely oblivious to choline block, then the values of the slowest open-time constant at infinitely high and infinitely low choline concentrations would be exactly those we predicted here (Fig. 4 A). The ~3,600 s^{-1} value for the choline dissociation rate from the transmitter binding sites of open diliganded AChRs is certainly reasonable considering the ~1,000-fold lower affinity of the open state for choline compared with that for ACh (for which this dissociation rate is <24 s^{-1}; Grosman and Auerbach, 2001). Thus, this alternative explanation for the prolongation of openings with increasing choline concentrations cannot be disregarded. A more careful examination follows.

Eqs. 14 and 15 give the time constant values of the longest-lived component of the open-time distribution at infinitely low and infinitely high concentrations of agonist, but the dependence of this time constant on the agonist concentration (i.e., its value at all the concentrations in between) cannot be expressed in a simple analytical form. Instead, the slowest open-time constant has to be computed numerically, at each agonist concentration, as the reciprocal of the smallest eigenvalue of the open-state submatrix ($-Q_{oo}$) of a pertinent kinetic scheme. To test whether the "open-state agonist-dissociation mechanism" could account for the experimental data in Fig. 4 A, we computed the eigenvalues of $-Q_{oo}$ (or the minus eigenvalues of Q_{oo}) from zero to 1 M choline, using the scheme in Fig. 13 as the kinetic model and assuming that choline block has no effect whatsoever on the kinetics of gating, entry into desensitization, or agonist binding/unbinding to/from the transmitter binding sites. The reciprocal of the smallest open-state eigenvalues are plotted in Fig. 14 (dashed line), along with the experimental observations from Fig. 4 A and the fit with Eq. 3 (solid line). It can be seen that, although both mechanisms predict an increase in the mean duration of observed openings as the concentration of choline increases, only Eq. 3 goes through the intermediate concentration data. Actually, the excellent fit of the experimental points with Eq. 3, which completely ignores the dissociation of ligand from the transmitter binding sites of OA_2 or OA_2B, strongly suggests that the contribution of the $2j_-$ term to the mean duration of choline-diliganded $OA_2 \rightleftharpoons OA_2B$ bursts is negligible. This implies that the dissociation

rate of choline from choline-diliganded open receptors is much slower than the value of ~3,600 s^{-1} discussed above, to the point that it can safely be ignored (see Eq. 14). The lower affinity of the open-state transmitter binding sites for choline, compared with that for ACh, could then be due to a slower association rate constant of choline to the open state. We firmly conclude that the lengthening of (apparent) openings with increasing choline concentrations is due to the slower closing rate constant of choline-blocked AChRs.

Choline is a quaternary-ammonium cation measuring ~5.5 Å along its longest axis (Fig. 15; for comparison, the diameter of a Na^+ or K^+ ion with a single hydration shell is ~7.5 Å). Its small size is certainly consistent with the hypothesis that this cation permeates the AChR (albeit at a much lower rate than Na^+ or K^+), but what is not at all obvious is how occupancy of a pore-blocking site (probably the selectivity filter itself) by such a small molecule can hamper the closure of the activation gate. This is not unprecedented, though; similar findings have been made in numerous other channels. Permeant ions retard the closure of the activation and inactivation gates in voltage-dependent K^+ and Na^+ channels (e.g., Swenson and Armstrong, 1981; Clay, 1986; Baukrowitz and Yellen, 1995; Townsend and Horn, 1997), whereas Ca^{2+} block speeds up the closure of the activation gate in voltage-dependent Na^+ channels (Armstrong and Cota, 1999), for example. In the case of the muscle AChR, the uncertainty as to the location and modes of operation of the activation (Unwin, 1995; Wilson and Karlin, 1998; Panicker et al., 2002; Miyazawa et al., 2003) and desensitization gates (Wilson and Karlin, 2001), combined with the lack of experimental information as to the precise location of the pore-blocking choline binding site(s), obscures any attempt to rationalize this phenomenon in structural terms. A "foot-in-the-door" type of mechanism (Armstrong, 1971), typically invoked to explain the effect of bulky quaternary-ammonium compounds on the closure of activation and inactivation gates in various ion channels, seems unlikely in the case of the smaller choline cation. Nevertheless, two concepts seem to emerge from our experimental data: (1) that the conformational changes that accompany gating (closed $\rightleftharpoons$ open) and desensitization (open $\rightleftharpoons$ desensitized) involve the rearrangement of different portions of the pore, and (2) that the desensitization gate can close "normally" even if closure of the activation gate is impeded. These conclusions seem broadly consistent with Karlin's findings in this regard (Wilson and Karlin, 2001), using the substituted-cysteine accessibility method, and with Auerbach's (Auerbach and Akk, 1998), using kinetic analysis of single-channel currents elicited in the presence of agonists other than choline. In both these cases, however, slower desensitization events were investigated (slower by, at least, a factor of ~10), and it is not clear whether the same "gate" can account for the different phases of desensitization.

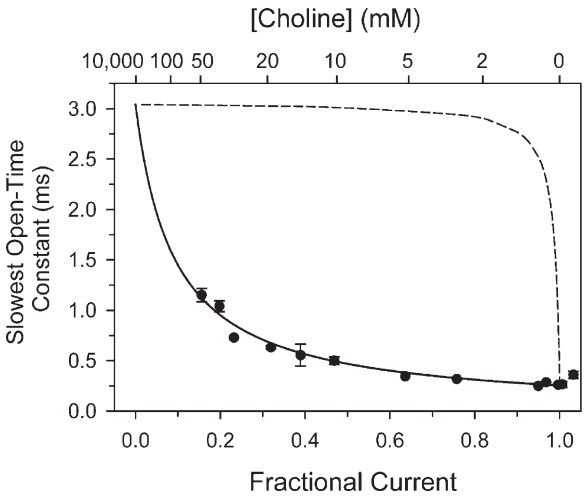

Figure 14. What causes the prolongation of (apparent) openings? The reciprocal of the smallest eigenvalues of the open-state $-Q_{oo}$ submatrix (i.e., the values of the slowest open-time constants) were numerically computed for the kinetic scheme in Fig. 13 at choline concentrations between zero and 1 M (dashed line). The figure also replots the data points in Fig. 4 A (i.e., the experimentally estimated values of the slowest open-time constants), along with the fit with Eq. 3 (solid line). It is evident that the "prolongation effect" of choline is due to a local effect of choline block on the closure of the activation gate (solid line), rather than to the increasing binding of choline to the open-state transmitter binding sites (dashed line). The shape of the dashed line plot largely depends on the values of the rate constants of diliganded-channel closing, entry into desensitization, and agonist association/dissociation to/from the open-state transmitter binding sites. The plot is rather insensitive to all other parameters in the kinetic scheme of Fig. 13 and to the assumption of equivalence and independence of the transmitter binding sites. It is interesting to realize that, as a general phenomenon in ligand-gated ion channels, the prolongation of open intervals with increasing ligand concentrations is not necessarily due to the slower closing rate constant of the open-blocked channel. As shown by the dashed line, the "open-state binding" hypothesis makes a comparable, yet clearly distinguishable, prediction.

Although this paper is likely to be the first time that the ability of choline block to slow down channel closure is characterized at a quantitative level, the observation that choline block lengthens the (apparent) open times has been consistently made since the introduction of choline as a tool in AChR structure–function studies (Grosman and Auerbach, 2000). Two other studies have also addressed the issue of the interaction between choline block and gating in the mouse muscle AChR (Akk and Steinbach, 2003; Akk et al., 2005), but these results led to the conclusion that choline block hastens the closure of the activation gate. We do not understand the reason for this marked discrepancy.

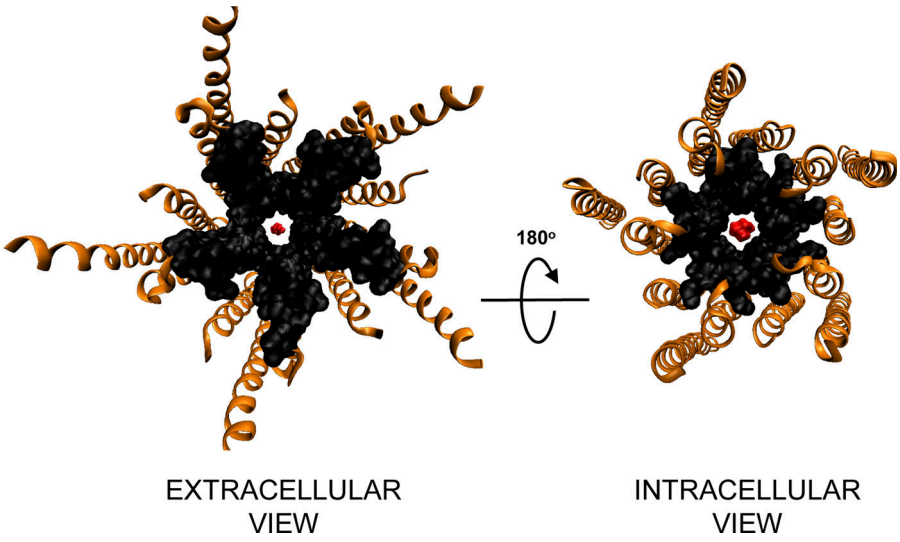

Figure 15. Relative dimensions of choline and the AChR's closed-channel pore. The five M2 segments (black) and a molecule of choline (red) are shown in surface representation (probe radius = 1.4 Å). The M1, M3, and M4 segments from the five subunits (orange) are shown in ribbon representation. Along the pore's longest axis, the choline molecule was positioned at the intracellular entrance of the pore, at the level of the selectivity filter (between the −2' and 2' positions of M2; Corringer et. al., 1999). Views from both the extracellular and the intracellular compartments are displayed. The protein atomic coordinates were taken from the PDB file 1OED (Miyazawa et al., 2003), a model of the transmembrane portion of the closed conformation of the *Torpedo* AChR. The atomic coordinates of choline were taken from the crystal structure of choline tetraphenylborate. The molecular image was made with VMD (Humphrey et al., 1996).

We thank Jagoda Jasielec and Jessica Gasser for technical assistance.

This work was supported by National Institutes of Health grant R01 NS042169 to C. Grosman.

Olaf S. Andersen served as editor.

Submitted: 18 October 2005
Accepted: 25 April 2006

REFERENCES

Adams, P.R. 1977. Voltage jump analysis of procaine action at the frog end-plate. *J. Physiol.* 268:291–318.

Akk, G., L.S. Milescu, and M. Heckmann. 2005. Activation of heteroliganded mouse muscle nicotinic receptors. *J. Physiol.* 564:359–376.

Akk, G., and J.H. Steinbach. 2003. Activation and block of mouse muscle-type nicotinic receptors by tetraethylammonium. *J. Physiol.* 551:155–168.

Armstrong, C.M. 1971. Interaction of tetraethylammonium ion derivatives with the potassium channels of giant axons. *J. Gen. Physiol.* 58:413–437.

Armstrong, C.M., and G. Cota. 1999. Calcium block of Na^+ channels and its effect on closing rate. *Proc. Natl. Acad. Sci. USA.* 96:4154–4157.

Auerbach, A., and G. Akk. 1998. Desensitization of mouse nicotinic acetylcholine receptor channels. A two-gate mechanism. *J. Gen. Physiol.* 112:181–197.

Baukrowitz, T., and G. Yellen. 1995. Modulation of K^+ current by frequency and external $[K^+]$: a tale of two inactivation mechanisms. *Neuron.* 15:951–960.

Carter, A.A., and R.E. Oswald. 1993. Channel blocking properties of a series of nicotinic cholinergic agonists. *Biophys. J.* 65:840–851.

Clay, J.R. 1986. Potassium ion accumulation slows the closing rate of potassium channels in squid giant axons. *Biophys. J.* 50:197–200.

Colquhoun, D., F. Dreyer, and R.E. Sheridan. 1979. The actions of tubocurarine at the frog neuromuscular junction. *J. Physiol.* 293:247–284.

Corringer, P.J., S. Bertrand, J.L. Galzi, A. Devillers-Thiéry, J.P. Changeux, and D. Bertrand. 1999. Mutational analysis of the charge selectivity filter of the α7 nicotinic acetylcholine receptor. *Neuron.* 22:831–843.

Croxen, R., C. Newland, D. Beeson, H. Oosterhuis, G. Chauplannaz, A. Vincent, and J. Newsom-Davis. 1997. Mutations in different functional domains of the human muscle acetylcholine receptor α subunit in patients with the slow-channel congenital myasthenic syndrome. *Hum. Mol. Genet.* 6:767–774.

Dwyer, T.M., D.J. Adams, and B. Hille. 1980. The permeability of the endplate channel to organic cations in frog muscle. *J. Gen. Physiol.* 75:469–492.

Edmonds, B., A.J. Gibb, and D. Colquhoun. 1995. Mechanisms of activation of muscle nicotinic acetylcholine receptors and the time course of endplate currents. *Annu. Rev. Physiol.* 57:469–493.

Franke, C., H. Parnas, G. Hovav, and J. Dudel. 1993. A molecular scheme for the reaction between acetylcholine and nicotinic channels. *Biophys. J.* 64:339–356.

Gardner, P. 1990. Nucleotide sequence of the ε subunit of the mouse muscle nicotinic receptor. *Nucleic Acids Res.* 18:6714.

Giraudat, J., M. Dennis, T. Heidmann, J.Y. Chang, and J.P. Changeux. 1986. Structure of the high-affinity binding site for noncompetitive blockers of the acetylcholine receptor: serine-262 of the δ subunit is labeled by [3H]chlorpromazine. *Proc. Natl. Acad. Sci. USA.* 83:2719–2723.

Grosman, C. 2003. Free-energy landscapes of ion-channel gating are malleable: changes in the number of bound ligands are accompanied by changes in the location of the transition state in acetylcholine-receptor channels. *Biochemistry.* 42:14977–14987.

Grosman, C., and A. Auerbach. 2000. Asymmetric and independent contribution of the second transmembrane segment 12' residues to diliganded gating of acetylcholine receptor channels: a single-channel study with choline as the agonist. *J. Gen. Physiol.* 115:637–651.

Grosman, C., and A. Auerbach. 2001. The dissociation of acetylcholine from open nicotinic receptor channels. *Proc. Natl. Acad. Sci. USA.* 98:14102–14107.

Grosman, C., M. Zhou, and A. Auerbach. 2000. Mapping the conformational wave of acetylcholine receptor channel gating. *Nature.* 403:773–776.

Hamill, O.P., A. Marty, E. Neher, B. Sakmann, and F.J. Sigworth. 1981. Improved patch-clamp techniques for high-resolution current recording from cells and cell-free membrane patches. *Pflugers Arch.* 391:85–100.

Humphrey, W., A. Dalke, and K. Schulten. 1996. VMD: visual molecular dynamics. *J. Mol. Graph.* 14:33–38.

Imoto, K., C. Busch, B. Sakmann, M. Mishina, T. Konno, J. Nakai, H. Bujo, Y. Mori, K. Fukuda, and S. Numa. 1988. Rings of negatively charged amino acids determine the acetylcholine receptor channel conductance. *Nature.* 335:645–648.

Jackson, M.B., B.S. Wong, C.E. Morris, H. Lecar, and C.N. Christian. 1983. Successive openings of the same acetylcholine receptor channel are correlated in open time. *Biophys. J.* 42:109–114.

Katz, B., and R. Miledi. 1978. A re-examination of curare action at the motor end-plate. *Proc. R. Soc. Lond. B. Biol. Sci.* 203:119–133.

Lee, B.S., R.B. Gunn, and R.R. Kopito. 1991. Functional differences among nonerythroid anion exchangers expressed in a transfected human cell line. *J. Biol. Chem.* 266:11448–11454.

Leffler, J.E., and E. Grunwald. 1963. Rates and equilibria of organic reactions. John Wiley & Sons, New York. 458 pp.

Legendre, P., D.W. Ali, and P. Drapeau. 2000. Recovery from open channel block by acetylcholine during neuromuscular transmission in zebrafish. *J. Neurosci.* 20:140–148.

Leonard, R.J., C.G. Labarca, P. Charnet, N. Davidson, and H.A. Lester. 1988. Evidence that the M2 membrane-spanning region lines the ion channel pore of the nicotinic receptor. *Science.* 242:1578–1581.

Maconochie, D.J., and J.H. Steinbach. 1995. Block by acetylcholine of mouse muscle nicotinic receptors, stably expressed in fibroblasts. *J. Gen. Physiol.* 106:113–147.

Miyazawa, A., Y. Fujiyoshi, and N. Unwin. 2003. Structure and gating mechanism of the acetylcholine receptor pore. *Nature.* 423:949–955.

Monod, J., J. Wyman, and J.-P. Changeux. 1965. On the nature of allosteric transitions: a plausible model. *J. Mol. Biol.* 12:88–118.

Neher, E., and J.H. Steinbach. 1978. Local anaesthetics transiently block currents through single acetylcholine-receptor channels. *J. Physiol.* 277:153–176.

Ogden, D.C., and D. Colquhoun. 1985. Ion channel block by acetylcholine, carbachol and suberyldicholine at the frog neuromuscular junction. *Proc. R. Soc. Lond. B. Biol. Sci.* 225:329–355.

Panicker, S., H. Cruz, C. Arrabit, and P.A. Slesinger. 2002. Evidence for a centrally-located gate in the pore of a serotonin-gated ion channel. *J. Neurosci.* 22:1629–1639.

Purohit, Y., and C. Grosman. 2006. Estimating binding affinities of the nicotinic receptor for low-efficacy ligands using mixtures of agonists and two-dimensional concentration–response relationships. *J. Gen. Physiol.* 127:719–735.

Qin, F. 2004. Restoration of single-channel currents using the segmental *k*-means method based on hidden Markov modeling. *Biophys. J.* 86:1488–1501.

Qin, F., A. Auerbach, and F. Sachs. 1996. Estimating single-channel kinetic parameters from idealized patch-clamp data containing missed events. *Biophys. J.* 70:264–280.

Sakmann, B., J. Patlak, and E. Neher. 1980. Single acetylcholine activated channels show burst-kinetics in the presence of desensitizing concentrations of agonist. *Nature.* 286:71–73.

Schwarz, G. 1978. Estimating the dimension of a model. *Ann. Statist.* 6:461–464.

Sine, S.M. 1993. Molecular dissection of subunit interfaces in the acetylcholine receptor: identification of residues that determine curare selectivity. *Proc. Natl. Acad. Sci. USA.* 90:9436–9440.

Sine, S.M., and J.H. Steinbach. 1984. Agonists block currents through acetylcholine receptor channels. *Biophys. J.* 46:277–283.

Swenson, R.P., Jr., and C.M. Armstrong. 1981. K^+ channels close more slowly in the presence of external K^+ and Rb^+. *Nature.* 291:427–429.

Townsend, C., and R. Horn. 1997. Effect of alkali metal cations on slow inactivation of cardiac Na^+ channels. *J. Gen. Physiol.* 110:23–33.

Unwin, N. 1995. Acetylcholine receptor channel imaged in the open state. *Nature.* 373:37–43.

van Wilgenburg, H., T. Piek, and P. Mantel. 1984. Ion channel block in rat diaphragm by the venom of the digger wasp Philantus triangulum. *Comp. Biochem. Physiol. C.* 79:205–211.

Wen, H., and P. Brehm. 2005. Paired motor neuron-muscle recordings in zebrafish test the receptor blockade model for shaping synaptic current. *J. Neurosci.* 25:8104–8111.

White, B.H., and J.B. Cohen. 1992. Agonist-induced changes in the structure of the acetylcholine receptor M2 regions revealed by photoincorporation of an uncharged nicotinic noncompetitive antagonist. *J. Biol. Chem.* 267:15770–15783.

Wilson, G.G., and A. Karlin. 1998. The location of the gate in the acetylcholine receptor channel. *Neuron.* 20:1269–1281.

Wilson, G.G., and A. Karlin. 2001. Acetylcholine receptor channel structure in the resting, open, and desensitized states probed with the substituted-cysteine-accessibility method. *Proc. Natl. Acad. Sci. USA.* 98:1241–1248.

Zhou, M., A.G. Engel, and A. Auerbach. 1999. Serum choline activates mutant acetylcholine receptors that cause slow channel congenital myasthenic syndromes. *Proc. Natl. Acad. Sci. USA.* 96:10466–10471.